Optimization
Iranian Journal of Optimization
Volume 15, Issue 4, 2023, 271-282
Research Paper

Online version is available on: https://sanad.iau.ir/journal/ijo

Islamic Azad University
Rasht Branch
ISSN: 2588-5723
E-ISSN:2008-5427

An Efficient Numerical Approach for Approximating Nonlocal Variable-Order Weakly Singular Integro-Differential Equations

Nayereh Tanha[1], Behrouz Parsa Moghaddam[2*] and Mousa Ilie[3]

[1] Department of Mathematics, Lahijan Branch, Islamic Azad University, Lahijan, Iran
[2*] Department of Mathematics, Lahijan Branch, Islamic Azad University, Lahijan, Iran
[3] Department of Mathematics, Rasht Branch, Islamic Azad University, Rasht, Iran

Revise Date: 27 November 2024
Accept Date: 05 December 2024

Keywords:
Fractional calculus
Variable-order fractional derivative
Fractional differential equations
Spline interpolation
Numerical optimization
Weakly singular integro-differential equation

Abstract

This paper presents an efficient numerical method for approximating variable-order fractional derivatives using an Integro spline quasi-interpolation approach. The proposed technique is extended to address nonlocal variable-order weakly singular integro-differential equations. Several illustrative examples are provided to validate the effectiveness and performance of the numerical scheme. Additionally, the optimal error orders are determined by minimizing the mean absolute error, demonstrating the method's accuracy and computational efficiency .

***Correspondence E-mail**: bparsa@iau.ac.ir

INTRODUCTION

Integro-differential equations have emerged as a powerful tool for describing complex phenomena over recent decades (Alawneh et al., 2010; Ahmad et al., 2021; Bakirova et al., 2021). These equations have found widespread applications in diverse fields, including physics, chemical kinetics, heat transfer, biological sciences, and viscoelasticity (MacCamy, 1977; Indiaminov et al., 2020; Durdiev & Rakhmonov, 2020; Abro et al., 2023). Various numerical methods have been developed to solve these equations, with notable approaches including Chebyshev collocation (Zeb et al., 2021), Chebyshev pseudospectral methods (Sunthrayuth et al., 2021), hat functions (Mohammed & Khudair, 2023), and Haar wavelets (Amin et al., 2021; Gürbüz, 2022).

The concept of variable-order fractional operators, also known as nonlocal variable-order operators, was first introduced by Samko and Ross (1993). These nonlocal operators are distinguished by their ability to preserve memory hereditary characteristics in dynamical systems. While fixed-order nonlocal operators characterize system memory using a uniform template, variable-order operators offer the flexibility to represent memory effects with varying templates. This has led to extensive research in both differential and integro-differential equations incorporating nonlocal operators of fixed and variable orders (Moghaddam & Machado, 2017; Mahdy, 2018; Mostaghim et al., 2018; Tuan et al., 2020; Amin et al., 2023).

We study the *nonlocal variable-order weakly singular integro-differential equation* (NVOWSIDE), which takes the form :

$$ {}^{v}\mathcal{D}_{0,t}^{\varrho(t)}u(t) = Q(t,u(t)) + P(t)\int_0^t \frac{u(\varsigma)}{(t-\varsigma)^{\beta(t)}}\,d\varsigma, \qquad (1) $$

$$ 0 < \beta(t) < 1, $$

with initial conditions :

$$ u^{(w)}(0) = u_w, \quad w = 0,1,\ldots,q-1, \qquad (2) $$

where q is a positive integer and the solution function $u(t)$ is assumed to possess continuous derivatives up to order $(q-1)$ .The function Q is defined as a jointly continuous mapping from $\Phi\times\mathbb{R}$ to $\mathbb{R}$,where Φ denotes the interval $[0,T]$ .Additionally, $P(t)$ represents a known continuous function on Φ . In this formulation, we utilize Variable-Order (VO) nonlocal operators, which were originally introduced by Caputo (1967) and subsequently expanded upon in Caputo (1969). These operators are characterized as follows:

Definition 1. The VO nonlocal derivative is stated as

$$ {}^{v}\mathcal{D}_{0,t}^{\varrho(t)}u(t) = \int_0^t \frac{(t-\varsigma)^{q-\varrho(t)-1}}{\Gamma(q-\varrho(t))}\cdot u^{(q)}(\varsigma)d\varsigma, \qquad (3) $$

$$ 0 \le q-1 < \varrho(t) \le q \in N, $$

and the VO nonlocal integral is stated as

$$ {}^{v}\mathcal{I}_{0,t}^{\varrho(t)}u(t) = \int_0^t \frac{(t-\varsigma)^{\varrho(t)-1}}{\Gamma(\varrho(t))}\cdot u(\varsigma)d\varsigma, \qquad (4) $$

$$ Re(\varrho(t)) > 0, $$

where $t,\varsigma \in R^{+}$ and $\Gamma(\cdot)$ denotes the Gamma function.

This research advances the field of numerical methods for NVOWSIDEs through three significant contributions. First, the study introduces novel numerical techniques that demonstrate enhanced computational accuracy and improved convergence order compared to current methodological approaches. Second, the research comprehensively examines the impact of different fractional orders on the mathematical modeling and solution of these complex differential equations. Third, the work systematically identifies and determines the optimal fractional orders that maximize computational efficiency and precision in NVOWSIDEs, thereby providing a robust methodological framework for researchers and practitioners working in this specialized domain.

The remainder of this paper is organized as follows. In Section 2, we present a novel and effective methodology for discretizing nonlocal operators through the application of integro spline quasi interpolation techniques. Section 3 serves two main purposes: first, we demonstrate the process of determining optimal Variable-orders through detailed analysis of two representative functions; second, we thoroughly investigate how

our proposed algorithms can be effectively applied to approximate NVOWSIDEs. Finally, Section 4 synthesizes our key findings, discusses the implications of our research, and presents our concluding remarks.

THEORETICAL RESULTS

In this section, we present a numerical approach to solve NVOWSIDE (1). For this purpose, let us consider a discrete time interval Φ where $t_m = m\Delta$ for $m = 0,1,..,M$. Here, Δ represents the uniform step size, and h denotes the size of each subinterval. The values of m and M are positive integers.

We define $\tau(t)$ as a quadratic polynomial on each subinterval $[t_j, t_{j+1}]$ where $0 = t_0 < t_1 < \ldots < t_m = T$. Specifically, $\tau(t)$ is referred to as an integro quadratic spline quasi-interpolant (IntQuaSpline-QI) function, constructed with respect to the given mesh points $t = [t_0, t_1, \ldots, t_m]$. Assuming that J_l represents the integral of $u(t)$ over each subinterval $[t_l, t_{l+1}]$, we can express this relationship as follows :

$$J_l = \int_{t_l}^{t_{l+1}} \tau(t)\mathrm{d}t = \int_{t_l}^{t_{l+1}} u(t)\mathrm{d}t,\ l = 0,1,\ldots,m-1, \quad (5)$$

then

$$\tau(t) = \frac{1}{12\Delta^3}((t-t_{l+1})^2\lambda_{l-2} - ((t-t_{l-1})(t-t_{l+1}) + (t-t_l)(t-t_{l+2}))\lambda_{l-1} + (t-t_l)^2\lambda_l), \quad (6)$$

where

$$\lambda_l = \begin{cases} 11J_0 - 7J_1 + 2J_2, l = -2, \\ 5J_0 + 2J_1 - J_2, \quad l = -1, \\ 8J_{l+1} - J_l - J_{l+2}, \ l = 0,\ldots,m, \\ \qquad\qquad m = 0,1,\ldots,M-3, \\ 5J_{m-1} + 2J_{m-2} - J_{m-3}, l = M-2, \\ 11J_{m-1} - 7J_{m-2} + 2J_{m-3}, l = M-1 \end{cases} \quad (7)$$

consequently, λ_l is solely determined by the integral values over the interval $[t_l, t_{l+3}]$.

Corollary 1 (Wu et al., 2020). [Assume $u(t) \in C^3(\Phi)$,hence

$$\| \partial_t^{(n)}\tau(t) - \partial_t^{(n)}u(t) \|_\infty = \mathcal{O}(\Delta^{3-n}), n = 0,1. \quad (8)$$

Corollary 2 (Wu et al., 2018). Assume $\Delta = \frac{T}{M}$, Φ is divided to m uniform sub-intervals and $u(t) \in C^\infty(\Phi)$, we have

$$\tau(t_l) = u(t_l) - \frac{h^4}{30}\partial_t^{(4)}u(t_l) + \textit{higher term}, \quad (9)$$

$l = 2,1,\ldots,m-2.$

and

$$\max_{2\le l\le m-2} |\tau(t_l) - u(t_l)| = \mathcal{O}(\Delta^4). \quad (10)$$

For the time points t_m , where $m = 1,...,M-1$, we have the following relationships :

$$\begin{aligned} {}^{v}\mathcal{D}_{0,t_m}^{\varrho(t)}u(t) &= \int_0^{t_m} \frac{(t_m-\varsigma)^{q-\varrho(t)-1}}{\Gamma(q-\varrho(t))}\cdot u^{(q)}(\varsigma)d\varsigma \\ &= \sum_{l=0}^{m-1}\int_{t_l}^{t_{l+1}} \frac{(t_m-\varsigma)^{q-\varrho(t)-1}}{\Gamma(q-\varrho(t))}\cdot u^{(q)}(\varsigma)d\varsigma, \end{aligned} \quad (11)$$

and

$$\begin{aligned} {}^{v}\mathcal{I}_{0,t_m}^{\beta(t)}u(t) &= \int_0^{t_m} \frac{u(\varsigma)}{(t_m-\varsigma)^{\beta(t)}}d\varsigma \\ &= \int_0^{t_m} \frac{u(\varsigma)}{(t_m-\varsigma)^{1-(1-\beta(t))}}d\varsigma \\ &= \sum_{l=0}^{m-1}\int_{t_l}^{t_{l+1}} \frac{u(\varsigma)}{(t_m-\varsigma)^{1-(1-\beta(t))}}d\varsigma. \end{aligned} \quad (12)$$

For each $l = 0,1,\ldots,m-1,$ we utilize an IntQuaSpline-QI function $\tau(t)$ with mesh points at t_l to approximate the function $u(t)$,resulting in the expressions:

$$\begin{aligned} u(t) \approx \tau_m(t) = \frac{1}{12\Delta^3}\sum_{l=0}^{m-1}&((t-t_{l+1})^2\lambda_{l-2} \\ &-((t-t_{l-1})(t-t_{l+1}) + (t-t_l)(t-t_{l+2}))\lambda_{l-1} \\ &+(t-t_l)^2\lambda_l) \end{aligned} \quad (13)$$

and

$$\begin{aligned} u^{(q)}(t) \approx \tilde{\tau}_m(t) = \frac{1}{12\Delta^3}\sum_{l=0}^{m-1}&((t-t_{l+1})^2\lambda_{l-2}^{(q)} \\ &-((t-t_{l-1})(t-t_{l+1}) \\ &+(t-t_l)(t-t_{l+2}))\lambda_{l-1}^{(q)} \\ &+(t-t_l)^2\lambda_l^{(q)}). \end{aligned} \quad (14)$$

By substituting Eq. (14) into Eq. (11), we obtain:

$$
\begin{aligned}
{}^{v}\mathcal{D}_{0,t_m}^{\varrho(t)}u(t) &\approx \sum_{l=0}^{m-1}\int_{t_l}^{t_{l+1}} \frac{(t_m-\varsigma)^{q-\varrho(t)-1}}{\Gamma(q-\varrho(t))}\tilde{\tau}_l(\varsigma)d\varsigma \\
&= \sum_{l=0}^{m-1}\int_{t_l}^{t_{l+1}} \frac{(t_m-\varsigma)^{q-\varrho(t)-1}}{12\Delta^3\Gamma(q-\varrho(t))}\Big((\varsigma-t_{l+1})^2\lambda_{l-2}^{(q)} \\
&-((\varsigma-t_{l-1})(\varsigma-t_{l+1})+(\varsigma-t_l)(\varsigma-t_{l+2}))\lambda_{l-1}^{(q)} \\
&+(\varsigma-t_l)^2\lambda_l^{(q)}\Big)d\varsigma.
\end{aligned} \tag{15}
$$

Moreover, by substituting Eq. (13) into Eq. (12), we obtain :

$$
\begin{aligned}
{}^{v}\mathcal{I}_{0,t_m}^{\beta(t)}u(t) &\approx \sum_{l=0}^{m-1}\int_{t_l}^{t_{l+1}} \frac{1}{(t_m-\varsigma)^{1-(1-\beta(t))}}\tilde{\tau}_l(\varsigma)d\varsigma \\
&= \sum_{l=0}^{m-1}\int_{t_l}^{t_{l+1}} \frac{1}{12\Delta^3(t_m-\varsigma)^{1-(1-\beta(t))}}\Big((\varsigma-t_{l+1})^2\lambda_{l-2} \\
&-((\varsigma-t_{l-1})(\varsigma-t_{l+1})+(\varsigma-t_l)(\varsigma-t_{l+2}))\lambda_{l-1} \\
&+(\varsigma-t_l)^2\lambda_l\Big)d\varsigma.
\end{aligned} \tag{16}
$$

Consequently, we derive the following propositions :

Proposition 1. Assume that $u(t)\in C^{q+4}(\Phi)$ be a function, $q-1<\varrho(t)\le q$ .The discretization of the nonlocal derivative can be stated from the IntQuaSpline-QI approximation as shown below

$$
\begin{aligned}
{}^{v}\mathcal{D}_{0,t_m}^{\varrho(t)}u(t) &= \sum_{l=0}^{m-1}\frac{\Delta^{q-\varrho_m-1}}{6\Gamma(q-\varrho_m+3)}(\alpha_{l,l-2}\lambda_{l-2}^{(q)} \\
&+\alpha_{l,l-1}\lambda_{l-1}^{(q)}+\alpha_{l,l}\lambda_l^{(q)}),
\end{aligned} \tag{17}
$$

where, for $l=0,1,\ldots,m$ λ_l , is defined in (7), and

$$
\alpha_{l,k}=\begin{cases}
-(m-l)^{q-\varrho_m+2} \\
+(\dfrac{(q-\varrho_m)^2}{2}+(2l-2m+1)\dfrac{q-\varrho_m}{2} \\
+(l-m)^2)(m-l+1)^{q-\varrho_m}, k=l-2, \\
(\dfrac{(q-\varrho_m)^2}{2}+(2m-2l+5)\dfrac{q-\varrho_m}{2} \\
-2(l-m)^2+(1+2l-2m))(m-l+1)^{q-\varrho_m} \\
+(-\dfrac{(q-\varrho_m)^2}{2} \\
+(2m-2l-3)\dfrac{q-\varrho_m}{2}+2(l-m)^2 \\
+(2m-2l-1))(m-l)^{q-\varrho_m}, k=l-1, \\
(-\dfrac{(q-\varrho_m)^2}{2}+(2l-2m-3)\dfrac{q-\varrho_m}{2}-(l-m)^2 \\
+(2l-2m-1))(m-l)^{q-\varrho_m} \\
+(m-l+1)^{q-\varrho_m+2}, k=l.
\end{cases} \tag{18}
$$

Proposition 2. Assume that $u(t)\in C^4(\Phi)$ be a function, $Re(\varrho(t))>0$. The discretization of the nonlocal integral can be stated from the IntQuaSpline-QI approximation as shown below

$$
\begin{aligned}
{}^{v}\mathcal{I}_{0,t_m}^{\beta(t)}u(t) &= \sum_{l=0}^{m-1}\frac{\Delta^{-\beta_m}\Gamma(1-\beta_m)}{6\Gamma(4-\beta_m)} \\
&(\nu_{l,l-2}\lambda_{l-2}+\nu_{l,l-1}\lambda_{l-1}+\nu_{l,l}\lambda_l),
\end{aligned} \tag{19}
$$

where, for $l=0,1,\ldots,m$ λ_l ,is defined in (7), and

$$
\nu_{l,k}=\begin{cases}
-(m-l)^{3-\beta_m}+(\dfrac{(1-\beta_m)^2}{2}+(2l-2m+1)\dfrac{1-\beta_m}{2} \\
+(l-m)^2)(m-l+1)^{1-\beta_m}, k=l-2, \\
(\dfrac{(1-\beta_m)^2}{2}+(2m-2l+5)\dfrac{1-\beta_m}{2} \\
-2(l-m)^2+(1+2l-2m))(m-l+1)^{1-\beta_m} \\
+(-\dfrac{(1-\beta_m)^2}{2}+(2m-2l-3)\dfrac{1-\beta_m}{2} \\
+2(l-m)^2+(2m-2l-1))(m-l)^{1-\beta_m}, \\
k=l-1, \\
(-\dfrac{(1-\beta_m)^2}{2}+(2l-2m-3)\dfrac{1-\beta_m}{2} \\
-(l-m)^2+(2l-2m-1))(m-l)^{1-\beta_m} \\
+(m-l+1)^{3-\beta_m}, k=l
\end{cases} \tag{20}
$$

Proposition 3. Let $u(t)\in C^{q+3}(\Phi)$ be a function, $q-1<\varrho(t)\le q$, and $\| \partial_t^{(q+3)}u(t)\|_\infty \le \Xi$, where $\Xi>0$ .Under these assumptions, the truncated error of presented algorithm is bounded, satisfying the following inequality :

$$AE_m = \| {}^{\nu}\mathcal{D}_{0,t_m}^{\varrho(t)}[u(t)] - \left({}^{\nu}\mathcal{D}_{0,t_m}^{\varrho(t)}[u(t)]\right)_{approx} \|_\infty \le \frac{\Xi m^{q-\varrho(t_m)}}{\Gamma(q-\varrho(t_m)+1)}\Delta^{q-\varrho(t_m)+3}. \quad (21)$$

Proof. Suppose $\tilde{\tau}_\Phi(t)$ is an IntQuaSpline-QI function that approximates $u(t)$ within the subinterval $[t_l,t_{l+1}]\subseteq\Phi$, where $l=0,1,...,m-1$. For an arbitrary value $\mu_l\in(t_l,t_{l+1})$, we can establish the following relationship :

$$\mathcal{E}_\Phi(t)=u^{(q)}(t)-\tilde{\tau}_\Phi^{(q)}(t)=\frac{\Delta^3}{12}\partial_t^{(q+3)}u(\mu_l),$$

thus

$$\begin{aligned}
&\| {}^{\nu}\mathcal{D}_{0,t_m}^{\varrho(t)}[u(t)] - \left({}^{\nu}\mathcal{D}_{0,t_m}^{\varrho(t)}[u(t)]\right)_{approx} \|_\infty \\
&= \| {}^{\nu}\mathcal{D}_{0,t_m}^{\varrho(t)}[u(t)] - {}^{\nu}\mathcal{D}_{0,t_m}^{\varrho(t)}[\tilde{\tau}_\Phi(t)] \|_\infty \\
&= \int_0^{t_m} \| \frac{(t_m-\varsigma)^{q-\varrho(t)-1}}{\Gamma(q-\varrho(t))}\mathcal{E}_\Phi(\varsigma)\|_\infty \, d\varsigma \\
&= \sum_{l=0}^{m-1}\int_{t_l}^{t_{l+1}} \frac{(t_m-\varsigma)^{q-\varrho(t)-1}}{\Gamma(q-\varrho(t))} \| \frac{\Delta^3}{12}\partial_t^{(q+3)}u(\mu_l)\|_\infty \, d\varsigma \\
&\le \frac{t_m^{q-\varrho(t_m)}\Xi}{\Gamma(q-\varrho(t_m)+1)}\Delta^3 = \frac{\Xi m^{\varrho(t_m)}}{\Gamma(q-\varrho(t_m)+1)}\Delta^{q-\varrho(t_m)+3}.
\end{aligned}$$

Proposition 4. Let $u(t)\in C^{q+4}(\Phi_1)$ be a function defined on the interval $\Phi_1=[t_2,t_{M-2}]\subseteq\Phi$ .Here, $q-1<\varrho(t)\le q$ and $\| \partial_t^{(q+4)}u(t)\|\infty\le\Xi_1$, where $\Xi_1>0$. Under these conditions, the truncated error of presented algorithm is bounded and can be expressed as follows :

$$\| {}^{\nu}\mathcal{D}_{0,t_m}^{\varrho(t)}[u(t)] - \left({}^{\nu}\mathcal{D}_{0,t_m}^{\varrho(t)}[u(t)]\right)_{approx} \|_\infty \le \frac{m^{q-\varrho(t_m)}\Xi_1}{\Gamma(q-\varrho(t_m)+1)}\Delta^{q-\varrho(t_m)+4}, \quad (22)$$

where $m=2,3,\ldots,M-3$.

Proof. Consider $\tilde{\tau}_{\Phi_1}(t)$ as an IntQuaSpline-QI function utilized to approximate $u(t)$ within the subinterval $[t_l,t_{l+1}]\subseteq\Phi$, where $l=2,3,...,m$. Hence, for any arbitrary value $\psi_l\in(t_l,t_{l+1})$, the following relation holds :

$$\begin{aligned}
&\mathcal{E}_{\Phi_1}(t)=u^{(q)}(t)-\tilde{\tau}_{\Phi_1}^{(q)}(t) \\
&=\frac{(t-t_l)^2(t-t_{l+1})^2}{30}\partial_t^{(q+4)}u(\psi_l),
\end{aligned}$$

hence

$$\begin{aligned}
&\| {}^{\nu}\mathcal{D}_{0,t_m}^{\varrho(t)}[u(t)] - \left({}^{\nu}\mathcal{D}_{0,t_m}^{\varrho(t)}[u(t)]\right)_{approx} \|_\infty \\
&= \| {}^{\nu}\mathcal{D}_{0,t_m}^{\varrho(t)}[u(t)] - {}^{\nu}\mathcal{D}_{0,t_m}^{\varrho(t)}[\tilde{\tau}_{\Phi_1}(t)] \|_\infty \\
&= \| \int_0^{t_m} \frac{(t_m-\varsigma)^{q-\varrho(t)-1}}{\Gamma(q-\varrho(t))}\mathcal{E}_{\Phi_1}(\varsigma)\|_\infty \, d\varsigma \\
&= \sum_{l=0}^{m-1}\int_{t_l}^{t_{l+1}} \frac{(t_m-\varsigma)^{q-\varrho(t)-1}}{\Gamma(q-\varrho(t))} \| \frac{(\varsigma-t_l)^2(\varsigma-t_{l+1})^2}{30}\partial_t^{(q+4)}u(\psi_l)\|_\infty \, d\varsigma \\
&\le \frac{t_m^{q-\varrho(t_m)}\Xi_1}{\Gamma(q-\varrho(t_m)+1)}\Delta^4 \\
&= \frac{m^{q-\varrho(t_m)}\Xi_1}{\Gamma(q-\varrho(t_m)+1)}\Delta^{q-\varrho(t_m)+4}.
\end{aligned}$$

Proposition 5. Let $u(t)\in C^3(\Phi)$ be a function, and $\| \partial_t^3 u(t)\|_\infty\le\chi$, where $\chi>0$. Under these assumptions, the truncated error of presented algorithm is bounded, satisfying the following inequality :

$$AE_m = \| {}^{\nu}\mathcal{I}_{0,t_m}^{\beta(t)}[u(t)] - \left({}^{\nu}\mathcal{I}_{0,t_m}^{\beta(t)}[u(t)]\right)_{approx} \|_\infty \le \frac{\chi m^{1-\beta(t_m)}}{1-\beta(t_m)}\Delta^{4-\beta(t_m)}. \quad (23)$$

Proof. Suppose $\tau_\Phi(t)$ is an IntQuaSpline-QI function that approximates $u(t)$ within the subinterval $[t_l,t_{l+1}]\subseteq\Phi$,where $l=0,1,...,m-1$. For an arbitrary value $\mu_l\in(t_l,t_{l+1})$, we can establish the following relationship :

$$\mathcal{E}_\Phi(t)=u(t)-\tau_\Phi(t)=\frac{\Delta^3}{12}\partial_t^3u(\mu_l),$$

thus

$$\left\| {}^{\nu}\mathcal{I}_{0,t_m}^{\beta(t)}[u(t)] - \left({}^{\nu}\mathcal{I}_{0,t_m}^{\beta(t)}[u(t)] \right)_{approx} \right\|_{\infty}$$
$$= \left\| {}^{\nu}\mathcal{I}_{0,t_m}^{\beta(t)}[u(t)] - {}^{\nu}\mathcal{I}_{0,t_m}^{\beta(t)}[\tau_{\Phi}(t)] \right\|_{\infty}$$
$$= \int_0^{t_m} \left\| (t_m - \varsigma)^{-\beta(t)} \mathcal{E}_{\Phi}(\varsigma) \right\|_{\infty} d\varsigma$$
$$= \sum_{l=0}^{m-1} \int_{t_l}^{t_{l+1}} (t_m - \varsigma)^{-\beta(t)} \left\| \frac{\Delta^3}{12} \partial_t^3 u(\mu_l) \right\|_{\infty} d\varsigma$$
$$\leq \frac{t_m^{1-\beta(t_m)} \chi}{1-\beta(t_m)} \Delta^3 = \frac{\chi m^{1-\beta(t_m)}}{1-\beta(t_m)} \Delta^{4-\varrho(t_m)}.$$

Proposition 6. Let $u(t) \in C^4(\Phi_1)$ be a function defined on the interval $\Phi_1 = [t_2, t_{M-2}] \subseteq \Phi$ .Here, $Re(\varrho(t)) > 0$ and $\| \partial_t^4 u(t) \| \infty \leq \chi_1$,where $\chi_1 > 0$. Under these conditions, the truncated error of presented algorithm is bounded and can be expressed as follows :

$$\| {}^{\nu}\mathcal{I}_{0,t_m}^{\beta(t)}[u(t)] - \left({}^{\nu}\mathcal{I}_{0,t_m}^{\beta(t)}[u(t)] \right)_{approx} \|_{\infty}$$
$$\leq \frac{m^{1-\beta(t_m)} \chi_1}{1-\beta(t_m)} \Delta^{5-\varrho(t_m)}, \quad (24)$$

where $m = 2,3,\ldots,M-3$.

Proof. Consider $\tau_{\Phi_1}(t)$ as an IntQuaSpline-QI function utilized to approximate $u(t)$ within the subinterval $[t_l, t_{l+1}] \subseteq \Phi$, where $l = 2,3,...,m$. Hence, for any arbitrary value $\psi_l \in (t_l, t_{l+1})$,the following relation holds :

$$\mathcal{E}_{\Phi_1}(t) = u(t) - \tau_{\Phi_1}(t) = \frac{(t-t_l)^2 (t-t_{l+1})^2}{30} \partial_t^4 u(\psi_l),$$

Hence

$$\left\| {}^{\nu}\mathcal{I}_{0,t_m}^{\beta(t)}[u(t)] - \left({}^{\nu}\mathcal{I}_{0,t_m}^{\beta(t)}[u(t)] \right)_{approx} \right\|_{\infty}$$
$$= \left\| {}^{\nu}\mathcal{I}_{0,t_m}^{\beta(t)}[u(t)] - {}^{\nu}\mathcal{I}_{0,t_m}^{\beta(t)}[\tau_{\Phi_1}(t)] \right\|_{\infty}$$
$$= \left\| \int_0^{t_m} (t_m - \varsigma)^{-\beta(t)} \mathcal{E}_{\Phi_1}(\varsigma) \right\|_{\infty} d\varsigma$$
$$= \sum_{l=0}^{m-1} \int_{t_l}^{t_{l+1}} (t_m - \varsigma)^{-\beta(t)} \left\| \frac{(\varsigma - t_l)^2 (\varsigma - t_{l+1})^2}{30} \partial_t^4 u(\psi_l) \right\|_{\infty} d\varsigma$$
$$\leq \frac{t_m^{1-\beta(t_m)} \chi_1}{1-\beta(t_m)} \Delta^4 = \frac{m^{1-\beta(t_m)} \chi_1}{1-\beta(t_m)} \Delta^{5-\varrho(t_m)}.$$

It is worth noting that if the values of $u^{(q)}(t_m), m = 0,1,\ldots,M$ are not available, we can apply the following backward finite difference quotient :

$$u^{(q)}(t_m) = \frac{1}{\Delta^q} \sum_{i=0}^{q} (-1)^i \binom{q}{i} u(t - i\Delta) + \mathcal{O}(\Delta), \quad (25)$$

where $q \in \mathbb{Z}^+$ is an arbitrary number and Δ represents the step size.

NUMERICAL DEMONSTRATIONS

Volterra integro-differential equations have found widespread applications across various scientific domains, as documented extensively in the literature. These applications span diverse phenomena, including diffusion processes, the formation of wind ripples in desert landscapes, heat transfer mechanisms, and neutron transport dynamics (Mandal & Chakrabarti, 2016). To validate the effectiveness of our proposed methodology, this section presents several carefully selected examples focusing on Nonlinear Variable-Order Weakly Singular Integro-Differential Equations (NVOWSIDEs). All numerical computations and simulations were performed using MATLAB version 2019 on a computing system equipped with an Intel (R) Core (TM) i7-8850 H processor operating at 2.60 GHz. To provide a comprehensive evaluation of our approach, we conduct detailed comparative analyses against existing numerical methods, examining both computational efficiency and solution accuracy. These comparisons serve to highlight the advantages and potential limitations of our proposed methodology in handling such complex mathematical systems.

A key objective of this research is to determine the optimal nonlocal variable-order (ONVO) that minimizes the mean absolute error (MAE). To evaluate the performance of our approach, we employ two crucial metrics: the mean absolute error ($\mathcal{E}_M$) and the convergence order (ECO), defined as follows:

$$\mathcal{E}_M = \sum_{m=1}^{M} \frac{AE_m}{M}, \tag{26}$$

$$ECO = \log_{\Delta}(\mathcal{E}_M). \tag{27}$$

The MAE serves as a measure of the average discrepancy between the numerical approximation and the exact solution, while the ECO quantifies the method's convergence rate. These metrics are calculated using the error formulations presented in Eq. (21) and (23), where AE_M represents the absolute difference between the exact and numerical solutions at each point, and M denotes the number of interior mesh points. To construct the ONVO for our examples, we consider two decreasing functions with several unknown parameters, specifically structured as follows.

$$\begin{cases} \varrho_1(t) = c_1 + c_2 t, \\ q-1 < c_1 < q, -1 < c_2 < 1 \\ \varrho_2(t) = c_3 + c_4 \exp(c_5 t), \\ q-1 < c_3 < q, -1 < c_4, c_5 < 1 \end{cases} \tag{28}$$

To determine the optimal values of the parameters c_i $(i = 1, 2, \cdots, 5)$, we employ a genetic optimization algorithm. The algorithm operates by minimizing the MAE across all discretized points for various step sizes Δ ,expressed mathematically as

$$Min \sum_{m=1}^{M} \frac{AE_m}{M}.$$

It is important to note that during this optimization process, the values of c_i are constrained to ensure that both functions $\varrho_1(t)$ and $\varrho_2(t)$ remain strictly bounded within the interval $(q-1, q)$. This constraint is essential for maintaining the mathematical validity and physical significance of our solution.

Example 1. Consider the NVOWSIDE

$$ {}^{v}\mathcal{D}_{0,t}^{\varrho(t)} u(t) = Q(t) + \int_0^t \frac{u(\zeta)}{(t-\zeta)^{\sin^2(t)}} d\zeta, \tag{29}$$

$$0 < \varrho(t) \le 1,$$

with initial condition $u(0) = 0$, where

$$Q(t) = \frac{t^{1+\cos^2(t)} - \sqrt{t}\, s_{\frac{3}{2}+\cos^2(t), \frac{1}{2}}(t)}{\cos^2(t)(1+\cos^2(t))} - \frac{\sqrt{t}\, s_{\frac{3}{2}-\varrho(t), \frac{1}{2}}(t) - t^{1-\varrho(t)}}{\Gamma(2-\varrho(t))} \tag{30}$$

and $s_{\mu,\nu}(t)$ is the Lommel function. It should be noted that $u(t) = \sin(t)$ is the exact solution of (29).

For Example 1, Table 1 presents the optimized values of coefficients c_i and the corresponding minimum MAE values for B-spline (Moghaddam & Machado, 2017) and proposed approachs, computed with parameters $q = 1$ and $\Delta = \frac{1}{32}$ over the interval $t \in [0, 2\pi]$. A comparative analysis between our proposed method, the B-spline approach (Moghaddam & Machado, 2017), and the exact solution is provided in Table 2. The results demonstrate that our numerical solutions exhibit excellent agreement with the exact solution. Furthermore, the proposed algorithm achieves superior accuracy compared to the B-spline method presented in (Moghaddam & Machado, 2017).

Table 1: The minimum values of MAE and optimal parameters of example 1 with $\varrho_1 = c_1 + c_2 t$ and $\varrho_2(t) = c_3 + c_4 \exp(c_5 t)$ for $\Delta = \frac{1}{32}$ in $t \in [0, 2\pi]$

MAE (Moghaddam et al. 2017)	MAE	c_1	c_2	c_3	c_4	c_5
1.60×10^{-4}	2.32×10^{-5}	0.16	-0.0008	0	0	0
1.70×10^{-4}	1.78×10^{-8}	0	0	0.5	0.001	0.00025

Table 2: Performance comparison between the B-spline method (Moghaddam & Machado, 2017)

and our developed algorithm for Example 1, showing maximum error ($\mathcal{E}_M$), convergence order (ECO), and computational time (in seconds). Results obtained using optimal variable-order functions $\varrho_1(t) = 0.16 - 0.0008t$ and $\varrho_2(t) = 0.5 + 0.01\exp(0.00025t)$ for various step sizes Δ over $t \in [0, 2\pi]$

		B-spline algorithm (Moghaddam & Machado, 2017)			Developed algorithm		
$\varrho(t)$	Δ	$\mathcal{E}_M$	ECO	$CPu\ time$	$\mathcal{E}_M$	ECO	$CPu\ time$
$\varrho_1(t)$	$\frac{1}{16}$	5.72×10^{-4}	2.69	2.686	4.57×10^{-5}	3.60	3.844
	$\frac{1}{32}$	1.60×10^{-4}	2.52	9.000	2.32×10^{-5}	3.08	14.562
	$\frac{1}{64}$	3.51×10^{-5}	2.48	36.030	1.17×10^{-5}	2.74	60.063
$\varrho_2(t)$	$\frac{1}{16}$	6.63×10^{-4}	2.64	2.594	2.17×10^{-7}	5.50	3.953
	$\frac{1}{32}$	1.70×10^{-4}	2.51	9.532	1.78×10^{-8}	5.13	16.156
	$\frac{1}{64}$	3.48×10^{-4}	2.48	2.047	4.23×10^{-9}	4.64	65.016

Fig. 1 illustrates two key comparisons for Eq. (29) with variable-order function $\varrho(t) = 0.5 + 0.01\exp(0.00025t)$ over the interval $t \in [0, 2\pi]$ using step size $\Delta = \frac{1}{32}$:the comparison between exact and approximate solutions obtained by our developed algorithm, and the logarithmic absolute errors ($\log_{10}(AE)$) for both our method and the B-spline approach (Moghaddam & Machado, 2017).

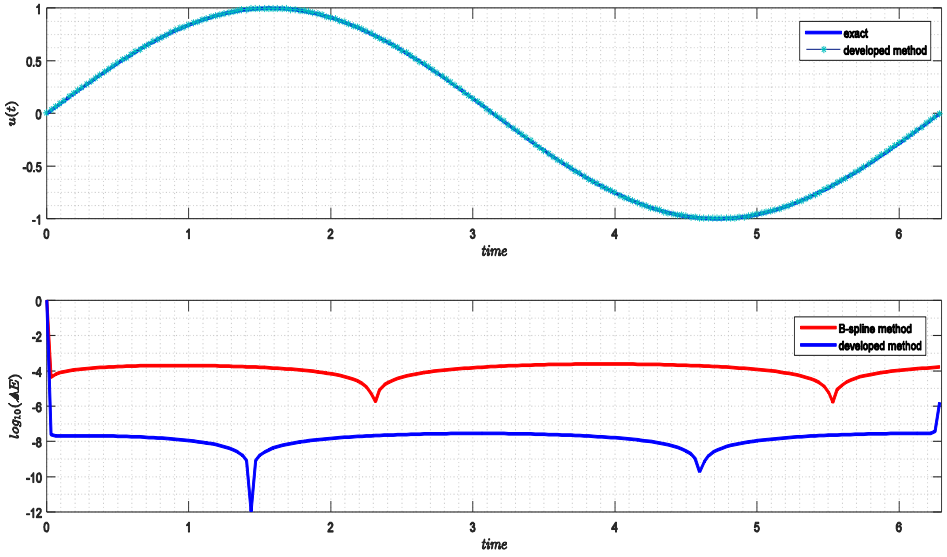

Fig. 1. (*Top panel*) Comparison of the numerical and exact solutions of (Moghaddam et al., 2021), (*Bottom panel*) magnitude of the $\log_{10}(AE)$,with the B-spline (Moghaddam & Machado, 2017) and proposed schemes, $\varrho(t) = 0.5 + 0.01\exp(0.00025t)$ and step size $\Delta = \frac{1}{32}$.

Example 2. Consider the NVOWSIDE

$$ {}^{v}\mathcal{D}_{0,t}^{\varrho(t)}u(t) = Q(t) + \int_0^t \frac{u(\zeta)}{(t-\zeta)^{\cos^2(t)}}\,d\zeta, \qquad (31) $$

$1 < \varrho(t) \le 2,$

with initial condition $u(0) = 0.25$,where

$$ Q(t) = -\frac{{}_2F_2\left([\frac{1}{2},1],[2-\frac{\varrho(t)}{2},\frac{3}{2}-\frac{\varrho(t)}{2}];-t^2\right)(\varrho^2(t)-7\varrho(t)+12)t^{2-\varrho(t)}}{2\Gamma(5-\varrho(t))} + \frac{{}_2F_2\left([\frac{3}{2},2],[3-\frac{\varrho(t)}{2},\frac{5}{2}-\frac{\varrho(t)}{2}];-t^2\right)t^{4-\varrho(t)}}{\Gamma(5-\varrho(t))} - \frac{{}_2F_2\left([\frac{1}{2},1],[1+\frac{\sin^2(t)}{2},\frac{1}{2}+\frac{\sin^2(t)}{2}];-t^2\right)t^{\sin^2(t)}}{4\sin^2(t)}, \qquad (32) $$

and ${}_sF_v(b_1,\ldots,b_s;a_1,\ldots,a_v;t)$ is the hypergeometric function. It should be noted that $u(t) = \frac{\exp(-t^2)}{4}$ is the exact solution of (31).

Following the analysis approach used in Example 1, Table 3 presents the optimized coefficients c_i and corresponding minimum MAE values for Example 2 for IQS-Moghaddam et al. (2021) and proposed approaches, computed with parameters $q = 2$ and $\Delta = \frac{1}{32}$ over $t \in [0,10]$ .Table 4 demonstrates that our method achieves superior accuracy compared to the IQS algorithm Moghaddam et al. (2021). Figure 2 provides a visual comparison for $\Delta = \frac{1}{32}$ with variable-order function $\varrho(t) = 1.63 - 0.1\exp(0.01t)$, displaying the logarithmic absolute errors ($\log_{10}(AE)$) of both our proposed method and the IQS approach Moghaddam et al. (2021) across the entire interval $t \in [0,10]$.

Table 3: The minimum values of MAE and optimal parameters of example 2 with $\varrho_1 = c_1 + c_2 t$ and $\varrho_2(t) = c_3 + c_4\exp(c_5 t)$ for $\Delta = \frac{1}{32}$ in $t \in [0,10]$

MAE (Moghaddam et al., 2021)	MAE	c_1	c_2	c_3	c_4	c_5
2.71×10^{-4}	1.89×10^{-6}	1.51	-0.001	0	0	0
3.21×10^{-4}	1.97×10^{-6}	0	0	1.63	0. 1	0.01

Table 4: Comparison of , and computational time (based on sec.) of 2 using the IQS- Moghaddam et al. (2021) and developed algorithms, with optimal values of $\varrho_1 = 1.51 - 0.001t$ and $\varrho_2(t) = 1.63 + 0.1\exp(0.01t)$ and Δ various values of in $t \in [0,10]$

		IQS algorithm Moghaddam et al. (2021)			Developed algorithm		
$\varrho(t)$	Δ	$\mathcal{E}_M$	*ECO*	*CPu time*	$\mathcal{E}_M$	*ECO*	*CPu time*
$\varrho_1(t)$	$\frac{1}{16}$	7.35×10^{-4}	2.59	22.562	3.11×10^{-6}	4.58	18.220
	$\frac{1}{32}$	2.71×10^{-4}	2.36	80.718	1.89×10^{-6}	3.80	78.938
	$\frac{1}{64}$	9.85×10^{-5}	2.22	350.188	9.73×10^{-7}	3.31	318.000
	$\frac{1}{16}$	8.69×10^{-4}	2.53	25.718	3.25×10^{-6}	4.54	19.968

		IQS algorithm Moghaddam et al. (2021)			Developed algorithm		
$\mathscr{e}_2(t)$	$\frac{1}{32}$	3.21×10^{-4}	2.32	91.938	1.97×10^{-6}	3.77	86.188
	$\frac{1}{64}$	1.21×10^{-4}	2.16	413.844	9.96×10^{-7}	4.58	18.220

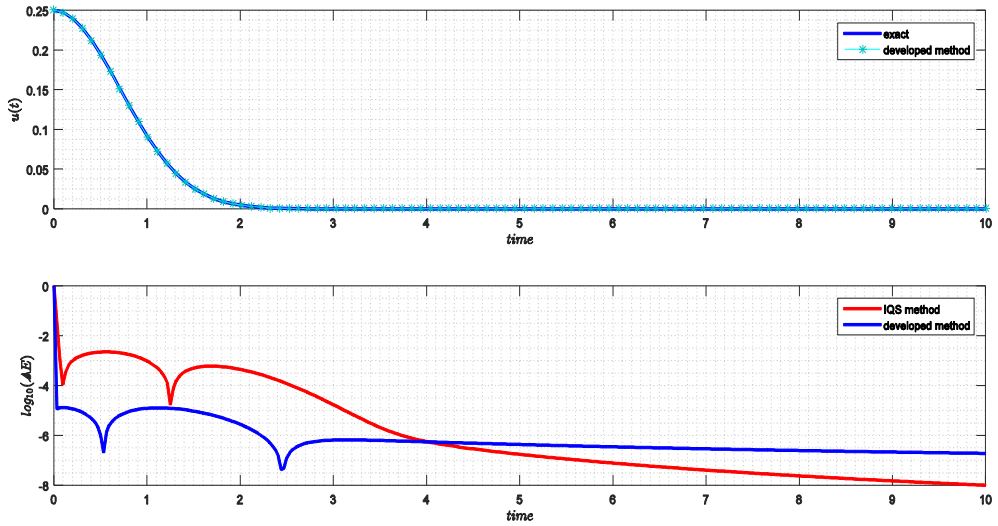

Fig. 2. (*Top panel*) Comparison of the numerical and exact solutions of (31), (*Bottom panel*) magnitude of the with the IQS- Moghaddam et al. 2021 and proposed schemes, and step size

CONCLUSION

This study has presented an efficient explicit numerical approach based on Integro spline quasi-interpolation for approximating variable-order fractional derivatives. The method was successfully extended to address nonlocal variable-order weakly singular integro-differential equations, offering a robust solution for complex fractional systems. Numerical results demonstrated the method's high accuracy, with optimal error rates achieved by minimizing the mean absolute error. The computational efficiency and precision of the proposed approach make it a valuable tool for solving fractional differential equations, particularly in scenarios involving nonlocal effects and weak singularities. Future research directions may include extending this method to broader classes of integro-differential equations and further optimizing its performance for large-scale problems.

REFERENCES

Abro, K. A., Atangana, A., & Gómez-Aguilar, J. F. (2023). A comparative analysis of plasma dilution based on fractional integro-differential equation: An application to biological science. *International Journal of Modelling and Simulation, 43*(1), 1–10. https://doi.org/10.1080/02286203.2021.2015818

Amin, R., Shah, K., Asif, M., Khan, I., & Ullah, F. (2021). An efficient algorithm for numerical solution of fractional integro-differential equations via Haar wavelet. *Journal of Computational and Applied Mathematics, 381*, 113028. https://doi.org/10.1016/j.cam.2020.113028

Amin, R., Sitthiwirattham, T., Hafeez, M. B., & Sumelka, W. (2023). Haar collocations method for nonlinear variable order fractional integro-differential equations. *Progress in Fractional Differentiation and Applications, 9*(2), 223–229. https://doi.org/10.18576/pfda/090203

Alawneh, A., Al-Khaled, K., & Al-Towaiq, M. (2010). Reliable algorithms for solving integro-differential equations with applications. *International Journal of Computer Mathematics*, *87*(7), 1538–1554. https://doi.org/10.1080/00207160802385818

Ahmad, J., Iqbal, A., & Mahmood, Q. H. U. (2021). Study of nonlinear fuzzy integrodifferential equations using mathematical methods and applications. *International Journal of Fuzzy Logic and Intelligent Systems*, *21*(1), 76–85. https://doi.org/10.5391/IJFIS.2021.21.1.76

Bakirova, E. A., Assanova, A. T., & Kadirbayeva, Z. M. (2021). A problem with parameter for the integro-differential equations. *Mathematical Modelling and Analysis*, *26*(1), 34–54. https://doi.org/10.3846/mma.2021.11977

Caputo, M. (1967). Linear models of dissipation whose Q is almost frequency independent-II. *Geophysical Journal International*, *13*(5), 529–539.

Caputo, M. (1969). Elasticità e dissipazione. Zanichelli.

Durdiev, D. K., & Rakhmonov, A. A. (2020). The problem of determining the 2D kernel in a system of integro-differential equations of a viscoelastic porous medium. *Journal of Applied and Industrial Mathematics*, *14*(2), 281–295. https://doi.org/10.1134/S1990478920020076

Gürbüz, B. (2022). A numerical scheme for the solution of neutral integrodifferential equations including variable delay. *Mathematical Sciences*, *16*(1), 13–21. https://doi.org/10.1007/s40096-021-00388-3

Indiaminov, R., Butaev, R., Isayev, N., Ismayilov, K., Yuldoshev, B., & Numonov, A. (2020). Nonlinear integro-differential equations of bending of physically nonlinear viscoelastic plates. *Materials Science and Engineering*, *869*(5), 052048. https://doi.org/10.1088/1757-899X/869/5/052048

Mandal, B. N., & Chakrabarti, A. (2016). *Applied singular integral equations*. CRC Press.

MacCamy, R. C. (1977). An integro-differential equation with application in heat flow. *Quarterly of Applied Mathematics*, *35*(1), 1–19. https://doi.org/10.1090/qam/452184

Mahdy, A. M. S. (2018). Numerical studies for solving fractional integro-differential equations. *Journal of Ocean Engineering and Science*, *3*(2), 127–132. https://doi.org/10.1016/j.joes.2018.05.004

Moghaddam, B. P., & Machado, J. A. T. (2017). A computational approach for the solution of a class of variable-order fractional integro-differential equations with weakly singular kernels. *Fractional Calculus and Applied Analysis*, *20*(4), 1023–1042. https://doi.org/10.1515/fca-2017-0053

Moghaddam, B. P., & Machado, J. A. T. (2017). SM-algorithms for approximating the variable-order fractional derivative of high order. *Fundamenta Informaticae*, *151*(1-4), 293–311. https://doi.org/10.3233/FI-2017-1493

Moghaddam, B. P., Mostaghim, Z. S., Pantelous, A. A., & Machado, J. A. T. (2021). An integro quadratic spline-based scheme for solving nonlinear fractional stochastic differential equations with constant time delay. *Communications in Nonlinear Science and Numerical Simulation*, *92*, Article ID 105475. https://doi.org/10.1016/j.cnsns.2020.105475

Moghaddam, B. P., Mostaghim, Z. S., Pishbin, M., Iyiola, O. S., Galhano, A., & Lopes, A. M. (2023). A numerical algorithm for solving nonlocal nonlinear stochastic delayed systems with variable-order fractional Brownian noise. *Fractal and Fractional*, *7*(4), Article ID 293. https://doi.org/10.3390/fractalfract7040293

Mostaghim, Z. S., Moghaddam, B. P., & Haghgozar, H. S. (2018). Computational technique for simulating variable-order fractional Heston model with application in US stock market. *Mathematical Sciences*, *12*, 277–283. https://doi.org/10.1007/s40096-018-0267-z

Sunthrayuth, P., Ullah, R., Khan, A., Shah, R., Kafle, J., Mahariq, I., & Jarad, F. (2021). Numerical analysis of the fractional-order nonlinear system of Volterra integro-differential equations. *Journal of Function Spaces*, *2021*(1), Article ID 1537958. https://doi.org/10.1155/2021/1537958

Tuan, N. H., Nemati, S., Ganji, R. M., & Jafari, H. (2020). Numerical solution of multivariable

order fractional integro-differential equations using the Bernstein polynomials. *Engineering with Computers*, *38*(Suppl 1), 139–147. https://doi.org/10.1007/s00366-020-01142-4

Wu, J., Ge, W., & Zhang, X. (2020). Integro spline quasi-interpolants and their super convergence. *Computational and Applied Mathematics*, *39*(3). https://doi.org/10.1007/s40314-020-01286-5

Wu, J., Shan, T., & Chungang, Z. (2018). Integro quadratic spline quasi-interpolants. *Journal of Systems Science and Mathematical Sciences*, *38*(12), 1407.

Zeb, H., Sohail, M., Alrabaiah, H., & Naseem, T. (2021). Utilization of Chebyshev collocation approach for differential, differential-difference and integrodifferential equations. *Arab Journal of Basic and Applied Sciences*, *28*(1), 413–426. https://doi.org/10.1080/25765299.2021.1997442